Intramolecular Disulfide Loop Formation in a Peptide Containing Two Cysteines†

Grayson H. Snyder
Department of Biological Sciences, State University of New York, Buffalo, New York 14260
Received August 22, 1986

ABSTRACT: The cyanogen bromide fragment comprising residues 115–181 of Kunitz soybean trypsin inhibitor is a soluble random-coil peptide at pH 7 containing two cysteines separated by eight other amino acids in the primary sequence. Four of the six rate constants have been determined for the three disulfide exchange reactions between this fragment and oxidized and reduced forms of *N*-acetylcysteine methyl ester. The rate constant for intramolecular loop formation in the fragment containing one thiolate anion and one sulfur connected by a disulfide bond to the small cysteine analogue is 0.36 ± 0.15 s^{-1} at 23 °C in 3 M guanidine hydrochloride. This measurement provides a frame of reference corresponding to formation of a small but sterically unstrained loop, the fast limit for intramolecular disulfide exchange in a random-coil peptide.

Quantitative evaluation of factors influencing formation of small disulfide-containing loops in proteins is important for understanding naturally occurring proteins involved in oxidation/reduction reactions and for developing strategies for designing novel synthetic polypeptide main frames having specific topologies. Proteins like thioredoxin, glutaredoxin, thioredoxin reductase, and protein disulfide isomerase participate in physiologically important disulfide exchange oxidation/reduction reactions. Each of these proteins contains one or more sequences of the type Cys-x-x-Cys[1] (O'Donnell & Williams, 1985; Edman et al., 1985; Klintrot et al., 1984). The local steric and chemical environments of the two proximate cysteines may play an important role in establishing the redox potential for the biochemical reactions which form and break a small disulfide loop between those cysteines. In bovine serum albumin, many of the domains are comprised of a sequence of the form Cys-x_m-Cys-Cys-x_m-Cys where the two central cysteines are immediately adjacent in the primary sequence (Dayhoff, 1978). Since steric constraints prevent the central cysteines from forming a disulfide with each other, this cluster forms an anchor for attachment of the two distant cysteines in the domain, thereby forming a topology of two loops attached at a common point. Such clusters might be included in protein engineering strategies for developing synthetic disulfide-cross-linked main frames. Functional proteins such as new enzyme inhibitors then might be constructed by adding appropriate residues to the sequence to give a protruding active amino acid on the main-frame's surface which is similar in character to an enzyme's natural substrate.

Cysteines separated by only a few residues in a polypeptide sequence may be unlikely to pair with each other, given steric constraints imposed in a small ring. For larger separations, random intramolecular collisions between cysteines are possible, with the probability of collision decreasing as the separation in the sequence increases (Kauzmann, 1959). Analysis of the products of complete air oxidation of peptides of the type Cys-glycine$_m$-Cys at low ionic strength (Heaton et al., 1956; Jarvis et al., 1961) revealed no intramolecular loop formation for m = 0 or 1, 15% and 40% loops for m = 2 and 3, respectively, and 90% or more loops for m = 4–6. These results partially reflect the influence of cysteine positioning on the equilibrium constant for intramolecular loop formation but are complicated by the significant extent of intermolecular disulfide formation promoted by the high peptide concentrations employed. Relative rate constants for reduction of the same series of monomers by reduced glutathione (Weber & Hartter, 1974) exhibit monotonically decreasing values as m is increased from 1 to 4. The rate constant for opening the small loop with m = 1 is 17 times faster than for the large loop with m = 4, possibly reflecting bond strain in the disulfide when m is small.

Figure 1 illustrates some of the reaction steps which may occur when a peptide containing two cysteines is combined with a small cysteine analogue.[2] A completely reduced (R) fragment may react with O–SS–O to form a species containing a single (S) mixed disulfide. This intermediate may form a loop (L) by intramolecular exchange, may react with another O–SS–O to form a species containing double (D) mixed disulfides, or may react with R to form a dimer. The numbers preceding the rate constants are statistical factors representing the different ways a particular step may occur. For example, conversion of R to S may occur four ways since either of the two SH groups on R may attack either of the two sulfurs on O–SS–O. At sufficiently low peptide concentrations, only the upper three reactions predominate. The six rate constants for these three reactions have been completely determined for a fragment of an immunoglobulin light chain containing two cysteines separated by about 60 positions in the primary sequence (Goto & Hamaguchi, 1981) under denaturing conditions in 8 M urea. This paper reports similar experiments on a protein fragment containing two cysteines separated by only eight residues. The values of the rate constants for loop formation (k_{SL}) determined for these two peptides then may be compared by using the theoretical prediction (Jacobsen & Stockmayer, 1950; Kauzmann, 1959) that k_{SL} is proportional

† This work was supported by National Institutes of Health Grant GM 26715.

[1] Abbreviations for the cyanogen bromide fragment comprising residues 115–181 of Kunitz soybean trypsin inhibitor: P, the peptide itself; R, reduced peptide; L, the form with an intramolecular disulfide loop; S and D, derivatives with single or double mixed disulfides. Other abbreviations: O–SH and O–SS–O, reduced and oxidized *N*-acetylcysteine methyl ester; Cys, cysteine; x, any amino acid; IAm, iodoacetamide; IOAc, iodoacetate; SCm, carboxymethylated sulfur group; SCam, carboxamidomethylated sulfur group; obsd, observed; subscript 0, initial; subscript EQ, equilibrium; av, average; Ig, immunoglobulin fragment; BPTI, bovine pancreatic trypsin inhibitor; DTT, dithiothreitol.

[2] Equilibrium constants are represented by an upper case K. Rate constants are represented by a lower case k. The first and second letters in the subscript correspond to a reactant and product, respectively.

0006-2960/87/0426-0688$01.50/0

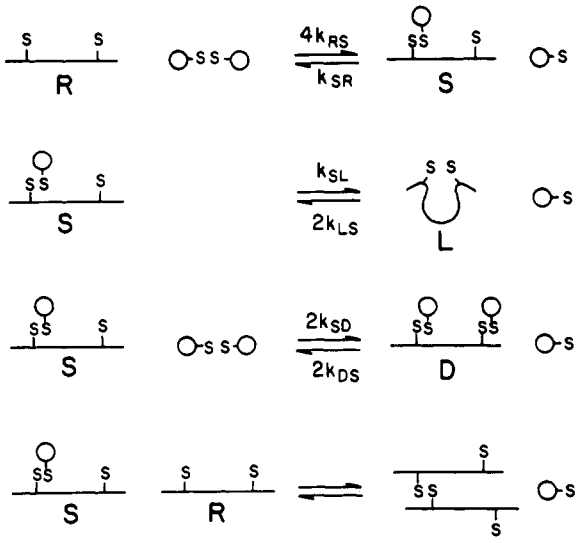

FIGURE 1: Disulfide exchange reactions between reduced and oxidized forms of soybean trypsin inhibitor fragment 115–181 and acetylcysteine methyl ester (O).

to $n^{-3/2}$, where $n - 1$ is the number of non-cysteine residues in the loop.

Experimental Procedures

Kunitz soybean trypsin inhibitor, iodoacetamide, and iodoacetate were obtained from Sigma Chemical Co. O–SS–O is supplied by Serva Fine Biochemicals. Sephadex gel filtration resins were obtained from Pharmacia Fine Chemicals.

IAm was purified by recrystallization from warm water to remove colored impurities. IOAc was purified by extracting an aqueous solution with carbon tetrachloride until the aqueous phase containing the IOAc became colorless. O–SS–O was purified by reverse-phase high-performance liquid chromatography using a water/acetonitrile gradient containing 0.1% trifluoroacetic acid. O–SH was prepared by reducing purified O–SS–O with thiopropyl-Sepharose 6B (Pharmacia Fine Chemicals) and isolating O–SH by reverse-phase chromatography using the same solvent gradiant. O–SH concentrations were determined both by gravimetric methods and by spectrophotometric assays of sulfhydryl groups using Ellman's reagent (Riddles et al., 1979). Since the results were identical, components of the liquid chromatography solvent do not bind to O–SH. Consequently, concentrations of O–SS–O isolated from the same solvent were determined gravimetrically. Soybean trypsin inhibitor was purified by previously published procedures (Yamamoto & Ikenaka, 1967; Frattali & Steiner, 1968). Subsequently, the carboxy-terminal cyanogen bromide fragment comprised of residues 115–181 and containing an intact disulfide bridge between cysteines-136 and -145 (species L) was isolated by published methods (Koide & Ikenaka, 1973) and further purified by reverse-phase chromatography using the solvent gradiant described above.

R was prepared by reducing L with dithiothreitol at pH 8.9 for 50 min at 40 °C, followed by acidification with glacial acetic acid, gel filtration on Sephadex G10, and lyophilization. Peptide concentration was determined by the absorbance at 280 nm using an estimated ϵ of 6756 M^{-1} cm^{-1} based on the sum of typical ϵ values (Mihalyi, 1969) for the one tryptophan and one tyrosine present in the peptide. Sulfhydryl concentrations were determined with Ellman's reagent. R routinely exhibited 1.9–2.1 SH groups per peptide by these assays.

An attempt to prepare D by reaction of R with 0.28 M O–SS–O in 3 M guanidine was unsuccessful. These conditions are close to the maximum solubility of O–SS–O. Rapid loop formation resulted in formation of mixtures of L and D which could not be separated by chromatographic methods.

Several derivatives of the peptide were prepared for use as gel electrophoresis standards. Oligomers were prepared by air oxidation of 1.8 mM peptide in a buffer containing 40 mM tris(hydroxymethyl)aminomethane, 0.5 μM Cu^{2+}, and 0.5 mM sodium azide adjusted to pH 8.5 and presaturated with O_2. Following overnight incubation at 23 °C, no free SH groups remained. The reaction mixture was desalted on Sephadex G10 and lyophilized. Subsequent gel filtration on Sephadex G100 gave two peaks corresponding to oligomer and L. The molecular weight of the oligomer corresponded to dimer, as determined by discontinuous gel electrophoresis using a published protocol for low molecular weight peptides (Swank & Munkres, 1971). Additional derivatives of the peptide containing two neutral –SCam groups or two negative –SCm groups were prepared by reacting 3×10^{-4} M R with 0.1 M IAm or IOAc, respectively. Reactions proceeded in 40 mM phosphate buffer at pH 7.1 and 23 °C for 5 min in the dark, prior to freezing and storing at −80 °C.

The pK_a value of the thiol group in glutathione or O–SH was determined by spectrophotometric titration at 245 nm (Benesch & Benesch, 1955). The sulfhydryl pK_a values in R were determined by monitoring the pH dependence of the kinetics of sulfhydryl group reaction with excess IAm, observing IAm disappearance at 265 nm (Finkle & Smith, 1958).

To determine rate constants and equilibrium constants for the disulfide exchange reactions, buffers were degassed and saturated with low-oxygen N_2 (Airco, Inc.). Stock solutions of sulfhydryl and disulfide-containing molecules were prepared in vials sealed with silicone septums (Pierce). Thiol prepared at pH 3 was injected into the disulfide solution with a gas-tight Hamilton syringe to initiate the exchange reaction. Final buffer conditions during the reaction were 3 M guanidine hydrochloride, 30 mM phosphate, and 1 mM ethylenediaminetetraacetic acid, pH 7.0 at 23 °C. At subsequent times, aliquots were withdrawn, and disulfide exchange was quenched by two methods. Some aliquots were quenched by lowering the pH to 3 with glacial acetic acid followed by freezing at −80 °C. When these control aliquots were thawed and assayed for –SH with Ellman's reagent, results indicated that there had been no net loss of –SH by reaction with possible residual O_2 in the nitrogen-containing vials. Other aliquots were quenched by 5-fold dilution into solutions containing IAm or IOAc to give final conditions of 0.1 M alkylating reagent in the same phosphate buffer. After reaction for 5 min at room temperature in the dark, these aliquots were frozen at −80 °C. At later times, these aliquots were desalted on small Sep-Pak reverse-phase C-18 cartridges (Millipore Corp.). Desalting was necessary to remove 3 M guanidine hydrochloride to obtain good behavior during subsequent gel electrophoresis. Peptides were obtained by elution with 0.1% trifluoroacetate in 40% acetonitrile, followed by lyophilization. Control experiments with mixtures of peptide derivatives demonstrated that all peptide species have equal affinities for the Sep-Pak cartridges under these conditions. Thus, the lyophilized desalted products contained the same relative concentrations of peptide species which were present in the quenched reaction mixtures applied to the cartridges.

These aliquots were analyzed by charge gels which differ from the standard Laemmli procedure (Laemmli, 1970) by the absence of sodium dodecyl sulfate or β-mercaptoethanol, the presence of 8 M urea, and a 17.5:1 acrylamide:bis(acrylamide) ratio. Slab gels 0.75 mm in thickness were stained with bromophenol blue and scanned at 633 nm using

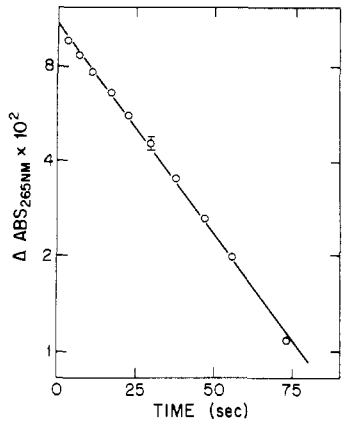

FIGURE 2: Kinetics of the reaction of R with IAm. $[R]_0 = 4.98 \times 10^{-5}$ M, $[IAm]_0 = 1.52 \times 10^{-3}$ M, 30 mM borate, 30 mM phosphate, 3 M guanidine hydrochloride, pH 10.65, $T = 22$ °C. The plotted curve is linear.

a helium–neon laser densitometer manufactured by LKB. Concentrations of individual peptide derivatives were determined by normalization of individual peak areas by the total integrated area of all peaks, and by knowing the total peptide in the original reaction mixture.

Results

The negative thiolate anion, $-S^-$, is the reactive form of cysteine in nucleophilic attack of disulfides and IAm. Thus, it is necessary to determine the sulfhydryl pK_a value in order to calculate the fraction of molecules which are participating in a reaction at a given experimental pH. For a simple isolated titrating group, this fraction is given by

$$f(S^-) = (1 + 10^{pK-pH})^{-1} \quad (1)$$

One method of determining the pK_a value is to monitor the pH dependence of the kinetics of reaction of a cysteine with excess IAm. Under these conditions, the kinetics will be pseudo first order with

$$k_{obsd} = k_{bimolecular}[IAm]f(S^-) \quad (2)$$

A plot of k_{obsd} vs. pH will be sigmoidal in shape, rising from a value of 0 at low pH where the –SH form predominates to some maximum value at high pH where $-S^-$ predominates. Figure 2 exhibits data for reaction of R with excess IAm at pH 10.65. The semilogarithmic plot is linear. Therefore, the two cysteines in R both must exhibit nearly the same k_{obsd} at this pH in 3 M guanidine hydrochloride. The experiment was repeated at pH 9.92, 8.90, and 8.43. Since the semilogarithmic plots were linear in all the experiments, these two cysteines have essentially identical pK_a values. Nonlinear least-squares analysis of titration data for R, glutathione, and O–SH gave respective pK_a values of 8.88 ± 0.07, 8.90 ± 0.06, and 8.58 ± 0.02 in this denaturing solvent. The values of bimolecular rate constants for reaction of R with IAm, reaction of $O–S^-$ with IAm, and reaction of $O–S^-$ with IOAc are 20.8 ± 0.8, 12.9 ± 1.0, and 10.1 ± 0.8 s^{-1} M^{-1}, respectively. The sulfhydryl groups in R and glutathione have similar pK_a values. The group in O–SH is chemically different, exhibiting a lower pK_a value and intrinsically lower reactivity with IAm. IAm and IOAc react with sulfhydryl groups with approximately similar velocities.

The relative mobilities of peptide derivatives on urea charge gels are given in Table I. Values for the four species with identical charge:mass ratios are 0.77 for the extended dimer Cam–S–P–SS–P–S–Cam, 0.82 for the compact looped dimer $P^{SS}_{SS}P$, 1.00 for each of the three extended monomers Cam–S–P–S–Cam, Cam–S–P–SS–O, and O–SS–P–SS–O, and 1.10 for the compact looped monomer P^{S}_{S}). This is consistent with the expected rank order of decreasing hydrodynamic volumes. The ratio of relative mobilities for extended dimers (0.87/0.77 = 1.13) is equal to the ratio of their charges (14–/12– = 1.17). This also is true for the extended monomers, having the ratios 7–/6– = 1.17 and 8–/6– = 1.33. The unmodified peptide behaves as though it has a net charge of 6–, which is consistent with expectations based on its amino acid composition, typical side-chain pK_a values, and an estimated running pH of 9.3 in the gel (Williams & Reisfeld, 1965). In disulfide exchange reactions in 3 M guanidine hydrochloride where the peptide concentration is less than 5×10^{-4} M, no oligomer formation is detected in the gels. Figure 3 includes normalized gel scans for a reaction converting L to S to R. The loss of L and the gain of R are readily apparent. R is measured from the peak at 1.33 in the IOAc series. If any D were present, it would be resolved at 1.00 in the IOAc gels. L is measured from the peak at 1.10 in the IAm series. Subtraction of its area from the combined areas of the partially overlapping L and S peaks in the IOAc gels gives a determination of the area corresponding to S.

Table I: Relative Mobilities on Urea Charge Gels

derivative		charge	$M_r \times 10^{-3}$	rel mobility
Cam–S–P–SS–P–S–Cam	IAm-quenched dimer[a]	12–	15.7	0.77
$P^{SS}_{SS}P$	O_2 oxidized dimer	12–	15.5	0.82
$^-$Cm–S–P–SS–P–S–Cm$^-$	IOAc-quenched dimer[a]	14–	15.7	0.87
Cam–S–P–S–Cam	IAm-quenched R	6–	7.9	1.00
Cam–S–P–SS–O	IAm-quenched S	6–	8.0	1.00
O–SS–P–SS–O	D	6–	8.1	1.00
P^{S}_{S}	L	6–	7.8	1.10
$^-$Cm–S–P–SS–O	IOAc-quenched S	7–	8.0	1.17
$^-$Cm–S–P–S–Cm$^-$	IOAc-quenched R	8–	7.9	1.33

[a] Obtained in reactions lacking guanidine.

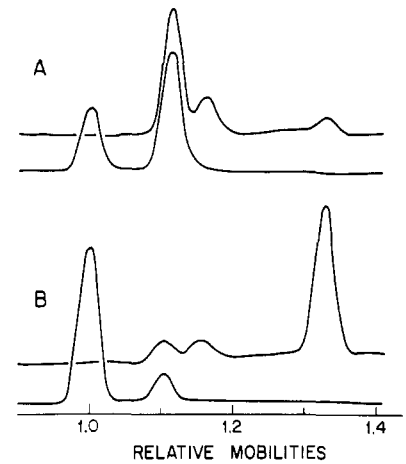

FIGURE 3: Gel scans of urea charge gels at 633 nm. $[L]_0 = 4.47 \times 10^{-5}$ M, $[O–SH]_0 = 1.86 \times 10^{-2}$ M, pH 6.83, $T = 23$ °C. Aliquots were quenched at (A) 0.75 and (B) 4.0 min. In each pair of scans, the upper trace = IOAc quenched aliquot and the lower trace = IAm quenched aliquot. Peak assignments are given in Table I.

Values for the rate constants k_{RS}, k_{SL}, and k_{SD} were obtained by oxidizing R with excess O–SS–O. Data are presented in Figure 4. Two independent experiments plotted as circles and triangles gave nearly identical results. As time increases, [R]

Table II: Rate Constants Determined by Numerical Integration[a]

rate constant	experiment 1[b]	2[c]	3[d]	4	av
k_{RS} (s^{-1} M^{-1})	27 ± 3	27 ± 3			27 ± 3
k_{SR} (s^{-1} M^{-1})			45 ± 5	37 ± 4	41 ± 9
k_{SL} (s^{-1})	0.39 ± 0.06	0.39 ± 0.06	0.33 ± 0.06	0.33 ± 0.06	0.36 ± 0.09
k_{LS} (s^{-1} M^{-1})			8.1 ± 0.9	9.9 ± 0.9	9.0 ± 1.6
k_{SD} (s^{-1} M^{-1})	6 ± 6				6 ± 6

[a] Errors indicate the extent to which rate constants can be varied without significantly affecting the quality of the fits. [b] Figure 4, circles and curves. [c] Figure 4, triangles. [d] Figure 5.

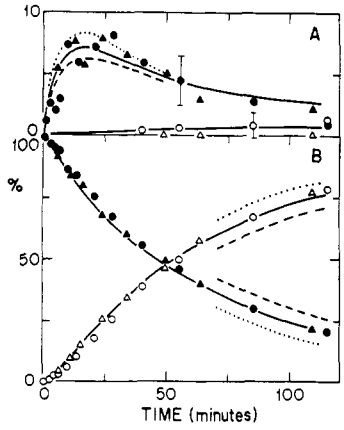

FIGURE 4: Kinetics of oxidation of reduced peptide by O–SS–O. $[R]_0 = 1.12 \times 10^{-4}$ M, $[O–SS–O]_0 = 4.08 \times 10^{-4}$ M, pH 6.68, $T = 23$ °C. Circles and triangles represent two independent experiments. (A) (○, △) Double; (●, ▲) single. (B) (○, △) Loop; (●, ▲) reduced. Curves are from numerical integration simulations using rate constants in Table II, as described in the text.

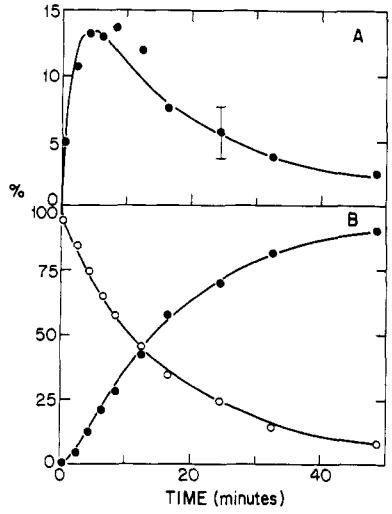

FIGURE 5: Kinetics of reduction of loop by O–SH. $[L]_0 = 4.32 \times 10^{-4}$ M, $[O–SH]_0 = 4.77 \times 10^{-3}$ M, pH 6.94, $T = 23$ °C. (A) (●) Single. (B) (○) Loop; (●) reduced. Double = zero at all time points. Curves are from numerical integration simulations.

decreases, S is transiently populated, and L accumulates. In one experiment, small amounts of D representing 0.5–1% of the total peptide were observed at late times. When the reaction was repeated, accumulation of D was too small to measure and was plotted as 0%. Errors in R, L, and D which appear at well-resolved positions in either the IOAc or the IAm gels are estimated as being ±1% of the total integrated area. The error in S, which is calculated by subtraction, consequently is twice that size. The magnitude of these errors is equal to the size of the symbols in Figure 4B and is given by error bars in Figure 4A.

The kinetic data were simulated by fifth-order Runge–Kutta–Fehlberg numerical integration (Danby, 1985). The simulation incorporated statistical factors from Figure 1. Thus, for example, prior to quenching

$$d[R]/dt = -4k_{RS}[R][O–SS–O]f(S^-)_{R–SH} + k_{SR}[S][O–SH]f(S^-)_{O–SH} \quad (3)$$

Simulations included both the period of time prior to addition of quenching reagent and the period of time following addition of an aliquot to IAm or IOAc. The extent of disulfide exchange occurring during quenching will be discussed later. Simulated concentrations at the end of quenching were used for comparison with gel data. The best fit is given by the solid lines in Figure 4. Sensitivity to a 20% increase or decrease in k_{RS} is given by dotted and dashed lines, respectively. Observed data for L and R lie well within these boundaries. Table II presents fitted values of the rate constants k_{RS}, k_{SL}, and k_{SD} determined in experiments 1 and 2. Simulated curves were insensitive to choices of k_{SR}, k_{LS}, and k_{DS}, corresponding to possible reverse steps in the reaction series. In this type of situation, final simulations used the average values determined in experiments 3 and 4 which are reported in the right-hand column in Table II. Thus, the curves in Figure 4 used 41 s^{-1} M^{-1} for k_{SR} and 9.0 s^{-1} M^{-1} for k_{LS}. The value of k_{DS} was not determined in any experiment. For final simulations, k_{DS} was assumed to be equivalent to k_{SR} and therefore was given a value of 41 s^{-1} M^{-1}.

Values for the rate constants k_{LS}, k_{SL}, and k_{SR} were obtained by performing the reaction in the opposite direction, reducing L with an excess of O–SH. Data for one such experiment are presented in Figure 5. Simulated fits were most sensitive to the bimolecular rate constants k_{LS} and k_{SR} but also exhibited dependence on the fast loop-forming step in the reverse direction governed by the intramolecular rate constant k_{SL}. Fits for data from a second repetition of the experiment required a 20% variation in k_{LS} and k_{SR}, as summarized in Table II. The value of k_{SL} (0.33 s^{-1}) obtained in experiments combining L with O–SH agrees within 20% of the value (0.39 s^{-1}) obtained when initial reactants are R and O–SS–O.

The average value of k_{SL} reported in Table II is 0.36 ± 0.09 s^{-1}. This error considers the sensitivity of fits to variation in k_{SL}. When one also includes uncertainties arising from the error in the sulfhydryl pK_a value (8.88 ± 0.07), the absolute magnitude of k_{SL} determined here is 0.36 ± 0.15 s^{-1}.

Equilibrium constants for the upper three reactions in Figure 1 were determined by using a large excess of O–SH and O–SS–O relative to P. These conditions generate a high percentage of the intermediate S at equilibrium. Furthermore, the concentrations of O–SH and O–SS–O at equilibrium may be approximated by their known initial values at time zero. Gel data for one reaction starting with L are given in Figure 6. Equilibrium is reached sometime between 2 min when [L] > [R] and 30 min when [L] < [R]. The straight lines are averages of gel areas for the last four time points. The disadvantage of using high concentrations of O–SH and O–SS–O

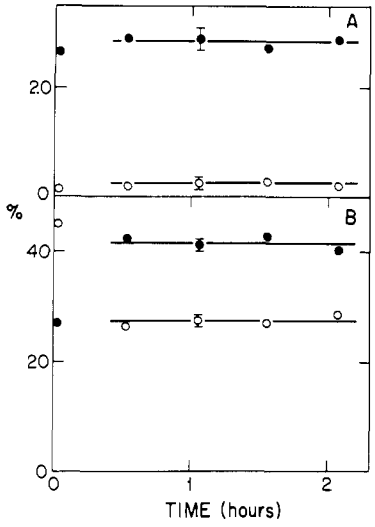

FIGURE 6: Determination of equilibrium concentrations. $[L]_0 = 1.00 \times 10^{-4}$ M, $[O\text{–}SH]_0 = 2.34 \times 10^{-2}$ M, $[O\text{–}SS\text{–}O]_0 = 1.00 \times 10^{-2}$ M, pH 6.88, $T = 23$ °C. (A) (○) Double; (●) single. (B) (○) Loop; (●) reduced. Lines are averages through equilibrium data.

Table III: Determination of Equilibrium Constants

equilibrium constant	ratio of equilibrium concn		ratio of rate constants
	expt 5[a]	expt 6	
K_{RS}	0.85 ± 0.08	0.78 ± 0.08	0.66 ± 0.21
K_{SL} (M)	0.054 ± 0.006	0.057 ± 0.006	0.040 ± 0.016
K_{SD}	0.42 ± 0.20	0.39 ± 0.13	

[a] Figure 6.

is an increase in the extent of disulfide exchange during quenching by IAm or IOAc. Numerical integrations employing the rate constants determined above indicate that the only significant effect occurs for equilibrium ratios corresponding to the loop-forming reaction. Here, $[L]_{EQ}/[S]_{EQ} = 0.76[L]_{GEL}/[S]_{GEL}$, where the subscript GEL represents equilibrium values for integrated areas from densitometer scans. Thus, using statistical factors in Figure 1, equilibrium exists when

$$k_{SL}[S]_{EQ}f(S^-)_{P\text{-}SH} = 2k_{LS}[L]_{EQ}[O\text{–}SH]_0 f(S^-)_{O\text{-}SH} \quad (4)$$

Equating equilibrium constants to ratios of intrinsic rate constants and incorporating the correction factor 0.76, one then obtains

$$K_{SL} = k_{SL}/k_{LS} = 2(0.76)[L]_{GEL}[O\text{–}SH]_0 f(S^-)_{O\text{-}SH}/[S]_{GEL}f(S^-)_{P\text{-}SH} \quad (5)$$

Values for the three intrinsic equilibrium constants calculated in this manner are given in Table III. The large uncertainty in K_{SD} arises from the small absolute magnitude of D and the correspondingly large fractional uncertainty in its concentration.

The equilibrium experiment in Figure 6 was repeated by using a 17% decrease in [O–SH]. The dependence of ratios of peptide concentrations on changes in [O–SH] and the ratio [O–SH]/[O–SS–O] can be predicted. For example, since $[L]_{EQ}[O\text{–}SH]/[S]_{EQ}$ is a constant, a 17% decrease in [O–SH] should cause a 17% increase in the ratio $[L]_{EQ}/[S]_{EQ}$. For each of the three equilibrium relationships, the peptide concentration ratios shifted in the predicted direction. The magnitude of the shift was consistent with expectations within experimental error. Values of equilibrium constants for the repeated experiment are reported in Table III and are within 10% of the values obtained originally. Furthermore, the values of equilibrium constants obtained from equilibrium concentrations agree within experimental error with values obtained by calculating the ratio of observed rate constants.

Discussion

Choice of Reagents. The cyanogen bromide fragment consisting of residues 115–181 of soybean trypsin inhibitor was selected for several reasons. First, its two cysteines are separated by only eight ($n - 1$) non-cysteine residues in the primary sequence. If it is correct that four to six intervening residues are optimal for facile sterically unrestricted loop formation (Heaton et al., 1956; Jarvis et al., 1961), the kinetics of loop formation in this species in 3 M guanidine should be close to the maximum rate that could be exhibited in a random-coil peptide. These experiments therefore should provide a useful frame of reference for consideration of the kinetics of steps in protein folding. Second, consideration of the peptide's average amino acid composition using a published hydrophobicity scale (Anastasious & Croxton, 1985) suggests that the fragment is more hydrophilic than polyglycine. The peptide has 26 charged groups at pH 7 distributed throughout the 66 amino acid sequence. The longest string of successive hydrophobic groups is five residues long. Peptide aggregation thus should be minimal. Circular dichroism studies (Toniolo et al., 1978) indicate that the fragment has a random-coil configuration in aqueous solutions at pH 7 and concentrations below 13 μM. Addition of 3 M guanidine should maintain this state. Finally, the peptide can be isolated by published procedures from an inexpensive commercially available protein.

Guanidine hydrochloride was chosen as a denaturing agent because its ionic nature would tend to minimize any differences in the pK_a values of the two cysteines of R caused by electrostatic differences in their local environments. O–SS–O was chosen as the linear oxidizing reagent instead of oxidized glutathione since it is smaller than glutathione and is electrostatically neutral. These two factors would tend to promote equivalent rate constants for reactions with the two cysteines of R, consistent with the model in Figure 1 used to fit kinetic data. A disadvantage of this choice is that the sulfhydryl group in O–SH is less like a protein's cysteines than the group in glutathione. The cysteine sulfur in O–SH has a slightly lower electron density. This is exhibited by the lower pK_a of O–SH (8.6) relative to R or gluuathione (both 8.9) and the lower rate constant for nucleophilic attack of IAm by $O\text{–}S^-$ (12.9 s^{-1} M^{-1}) relative to attack of IAm by $R\text{–}S^-$ (20.8 s^{-1} M^{-1}). The pK_a of a cysteine and the rate constant for its participation in nucleophilic substitutions both reflect the influence of neighboring groups on the electron density at the sulfur (Szajewski & Whitesides, 1980).

Validity of the Model. Use of the model presented in Figure 1 requires equivalence of the two cysteines of R and a lack of oligomer formation. Use of 3 M guanidine prevents formation of oligomers which would appear in gels with relative mobilities less than 1.00, as recorded in Table I. The linear nature of semilogarithmic plots of the type presented in Figure 2 indicates that the two sulfhydryl groups react with the small neutral molecule IAm with nearly identical rate constants. Calculations employing computer-generated data suggest that nonlinearity would be apparent if the two rate constants differed by more than a factor of 2.5. However, nonlinearity would be difficult to detect if the rate constants differed, but only by a factor of 1.5 or less. If equivalence exists in reactions with the larger molecules O–SH and O–SS–O, then identical values should be obtained for the two intrinsic equilibrium constants K_{RS} and K_{SD} and for the two intrinsic rate constants k_{RS} and k_{SD}. K_{RS} (0.8 ± 0.1) and K_{SD} (0.4 ± 0.2) determined from equilibrium concentrations appear to differ by a factor

Table IV: Comparison of Rate Constants for Loop Formation

solvent	pH	leaving group	n	$k_{SL,obsd}$ (s^{-1}) calcd for P	$k_{SL,obsd}$ (s^{-1}) obsd
3 M guanidine	7.0	O–SH	9		0.0047 (P)
3 M guanidine	8.1	O–SH	9	0.051	
3 M guanidine	8.1	glutathione	9	0.030	
8 M urea	8.1	glutathione	9	0.022	
8 M urea	8.1	glutathione	60	0.0013	0.001 (Ig)

of 2. The rate constants k_{RS} (27 ± 3 s^{-1} M^{-1}) and k_{SD} (6 ± 6 s^{-1} M^{-1}) appear to differ by a factor of 4 but could easily be identical within a factor of 2. Low values of measurable D introduce significant uncertainty into these comparisons. Some nonequivalence may exist for the two cysteines of P. Thus, it is possible that the loop-closing reaction to be considered below occurs most often with an S species where a particular one of the two cysteines comprises the thiolate anion and the other cysteine comprises the mixed disulfide.

Comparison of k_{SL} Values for Different Denatured Peptides. There has been one other complete kinetic study of loop formation in a two-cysteine protein fragment under denaturing conditions (Goto & Hamaguchi, 1981). This work considered reactions of glutathione with an immunoglobulin light-chain fragment comprised of about 100 residues, having 2 cysteines separated by about 60 positions in the sequence. At pH 8.1 in 8 M urea, $k_{SL,obsd}$ was 0.001 s^{-1}. Table IV summarizes attempts to estimate the value of $k_{SL,obsd}$ for P under similar conditions. First, the observed value of 0.0047 s^{-1} at pH 7 (corresponding to 0.36 s^{-1} for completely ionized S^-) is corrected to 0.051 s^{-1} at pH 8.1 by using eq 1 and 2. Then the kinetics of intramolecular attack of P–SS–O and P–SS–glutathione disulfides by a P–SH group should be related by [eq 36 of Szajewski & Whitesides (1980)]

$$\log k_{\text{disulfide exchange}} = \text{constant} - 0.73 p K_{a,\text{leaving group}} \quad (6)$$

where O–S^- and glutathione are the respective leaving groups. Using the pK_a values determined above, one then calculates that the observed k with acetylcysteine methyl ester would be 1.7-fold slower (0.030 s^{-1}) if a glutathione-like group had been used. Fluorescence resonance energy-transfer studies have indicated that for $n = 8$ or larger, the diffusion coefficient describing the relative motions of the two ends of an oligopeptide chain is inversely proportional to solvent viscosity (Haas et al., 1978; Cerf, 1979). The viscosities of 3 M guanidine and 8 M urea relative to pure water at 25 °C are 1.17 and 1.60, respectively (Kawahara & Tanford, 1966). Thus, both intermolecular and intramolecular collisions are predicted to be 1.4-fold slower (1.60/1.17) in 8 M urea than observed here. Finally, one considers the dependence of k on loop size. If n is sufficiently large to facilitate sterically unrestricted loop formation, k_{SL} should be approximately proportional to $n^{-3/2}$ (Jacobsen & Stockmayer, 1950; Kauzmann, 1959). Thus, the value of 0.022 s^{-1} for $n = 9$ is equivalent to a $(60/9)^{3/2}$ or a 17-fold lower value of 0.0013 s^{-1} for $n = 60$. As summarized in Table IV, this is close to the observed value of 0.001 s^{-1} in the immunoglobulin fragment. These two studies, therefore, are consistent with each other regarding the time frame of loop formation in sterically unrestricted random-coil two-cysteine peptides.

In principle, it may be possible to obtain an estimate for k_{SL} based on studies of the oxidation of reduced bovine pancreatic trypsin inhibitor by the cyclic disulfide oxidized dithiothreitol, at pH 8.7 in 8 M urea (Creighton, 1977). Reduced pancreatic trypsin inhibitor has six cysteines separated by a variety of distances within the primary sequence. Formation of a loop is given by

$$\text{BPTI-(SH)}_6 + \text{DTT}^{\text{S}}_{\text{S}} \overset{6K_{DTT}}{\rightleftharpoons} \text{(HS)}_5\text{-BPTI-SS-DTT-SH} \overset{5k_{SL,av}}{\rightarrow} \text{(HS)}_4\text{-BPTI}^{\text{S}}_{\text{S}} + \text{DTT-(SH)}_2 \quad (7)$$

In this case, it is not possible to isolate the mixed disulfide intermediates. Formation of the set of species containing one disulfide is given by

$$k_{obsd} = 6K_{DTT}(5k_{SL,av}) = 2K_{DTT}(15k_{SL,av}) = 2K_{DTT}\sum k^i_{SL} \quad (8)$$

where $i = 15$, the number of possible single disulfide species. It recently has been suggested (Creighton & Goldenberg, 1984) that the best way to evaluate data for the trypsin inhibitor studies at pH 8.7 is to equate k_{SL} to the glutathione-like rate constant, incorporate the statistical factors in eq 8, and then use a value of $(600\ M)^{-1}$ for K_{DTT} at that pH. From the value $k_{obsd} = 0.016$ s^{-1} M^{-1} (Creighton, 1977), one then obtains $k_{SL,av} = 0.32$ s^{-1}. When a typical value of $pK_a = 8.9$ as above is used, this gives $k_{SL,av} = 0.11$ s^{-1} at pH 8.1. In this protein, 1 of the 15 possible disulfides has $n = 4$, and all others have $n \geq 8$. The average value of n is 25, but the appropriately weighted average for consideration here is $n_{av} = 13$, where $n_{av}^{-3/2} = (1/15)\sum n_i^{-3/2}$. This weighting emphasizes smaller values of n associated with the faster kinetic processes expected to dominate the observed data. One then estimates that $k_{SL,av}$ would be $(60/13)^{3/2}$ smaller or 0.011 s^{-1} for $n = 60$. Thus, even after decreasing k_{obsd} by a factor of 30 to account for statistical factors, the estimate of $k_{SL,av}$ remains an additional 10 times faster than the time frame suggested by studies of the two-cysteine fragments in Table IV. The latter studies may provide a more reliable estimate. Their data are easier to interpret since k_{SL} is derived from changes in directly observed concentrations of a mixed disulfide species forming a loop of only one possible size.

Efficiency of Quenching. It is useful to compare the time required for quenching SH by IAm or IOAc with the time frames of disulfide exchange. The intramolecular loop formation step at pH 7.0 in the original reaction mixture exhibits a $\tau = 3.6$ min $= [k_{SL} f(S^-)_{P\text{-}SH}]^{-1}$. In kinetic experiments, the fastest reaction of peptide with O–SS–O corresponds to conversion of R to S given in Figure 4 and exhibits a $\tau = 29$ min $= [4k_{RS}[\text{O–SS–O}] f(S^-)_{P\text{-}SH}]^{-1}$. Similarly, the fastest reaction of peptide with O–SH corresponds to conversion of S to R in the experiment presented in Figure 5, exhibiting a $\tau = 3.3$ min $= [k_{SR}[\text{O–SH}] f(S^-)_{O\text{-}SH}]^{-1}$. Following 5-fold dilution into IAm, the two intermolecular τ values are increased 5-fold to 145 and 17 min, respectively. The intramolecular τ remains the same. In 0.1 M IAm, the irreversible quenching of a peptide SH is given by $\tau = 0.62$ min $= [f(S^-)_{P\text{-}SH}[\text{IAm}](20.8\ s^{-1}\ M^{-1})]^{-1}$. Quenching of O–SH is given by $\tau = 0.50$ min $= [f(S^-)_{O\text{-}SH}[\text{IAm}](12.9\ s^{-1}\ M^{-1})]^{-1}$. Thus, in the quenching solution, all SH disappears on a time frame of 0.6 min, loop formation occurs on a time frame which is 6-fold slower (3.6 min), and all bimolecular disulfide exchange processes have been made relatively insignificant by dilution of the original reaction mixture. Thus, about $^6/_7$ of S is quenched, but $^1/_7$ of S converts to L during the quenching process. In the above experiments, this was considered by experimentally determining the rate constants for reaction with IAm or IOAc and then extending the numerical integration simulations into the quenching process. The choice of 0.1 M for the concentration of IAm or IOAc was used both in these studies and in the experiments with pancreatic trypsin inhibitor and the immunoglobulin fragment. In future experiments, the concentrations of quenching reagent probably should be increased to 0.4 M to minimize reliance on computer simulations. This will be

possible, since control experiments indicate that the limiting solubility of both IAm and IOAc is greater than 1.0 M in 3 M guanidine hydrochloride at pH 7.

ACKNOWLEDGMENTS

I appreciate the technical assistance of Yiping Sun.

Registry No. IAm, 144-48-9; IOAc, 64-69-7; *N,N'*-diacetylcystine dimethyl ester, 32381-28-5; *N*-acetylcysteine methyl ester, 7652-46-2; cysteine, 52-90-4.

REFERENCES

Anastasiou, N., & Croxton, C. A. (1985) *J. Biomol. Struct. Dyn. 2*, 871–878.

Benesch, R. E., & Benesch, R. (1955) *J. Am. Chem. Soc. 77*, 5877–5881.

Cerf, R. (1979) *Biopolymers 18*, 731–734.

Creighton, T. E. (1977) *J. Mol. Biol. 113*, 313–328.

Creighton, T. E., & Goldenberg, D. P. (1984) *J. Mol. Biol. 179*, 497–526.

Danby, J. M. A. (1985) in *Computing Applications to Differential Equations*, pp 1–52 and 245–246, Reston Publishing Co., Reston, VA.

Dayhoff, M. O. (1978) in *Atlas of Protein Sequence and Structure*, Vol. 5, Supplement 3, National Biomedical Research Foundation, Silver Spring, MD.

Edman, J. C., Ellis, L., Blacher, R. W., Roth, R. A., & Rutter, W. J. (1985) *Nature (London) 317*, 267–270.

Finkle, B. J., & Smith, E. L. (1958) *J. Biol. Chem. 230*, 669–690.

Frattali, V., & Steiner, R. F. (1968) *Biochemistry 7*, 521–530.

Goto, Y., & Hamaguchi, K. (1981) *J. Mol. Biol. 146*, 321–340.

Haas, E., Katchalski-Katzir, E., & Steinberg, I. Z. (1978) *Biopolymers 17*, 11–31.

Heaton, G. S., Rydon, H. N., & Schofield, J. A. (1956) *J. Chem. Soc.*, 3157–3168.

Jacobson, H., & Stockmayer, W. H. (1950) *J. Chem. Phys. 18*, 1600–1606.

Jarvis, D., Rydon, H. N., & Schofield, J. A. (1961) *J. Chem. Soc.*, 1752–1756.

Kauzmann, W. (1959) in *Sulfur in Proteins* (Benesch, R., Benesch, R. E., Boyer, P. D., Klotz, I. M., Middlebrook, W. R., Szent-Gyorgyi, A. G., & Schwarz, D. R., Eds.) pp 93–108, Academic Press, New York.

Kawahara, K., & Tanford, C. (1966) *J. Biol. Chem. 241*, 3228–3232.

Klintrot, I. M., Hoog, J. O., Jornvall, H., Holmgren, A., & Luthman, M. (1984) *Eur. J. Biochem. 144*, 417–423.

Koide, T., & Ikenaka, T. (1973) *Eur. J. Biochem. 32*, 401–407.

Laemmli, U. K. (1970) *Nature (London) 227*, 680–685.

Mihalyi, E. (1969) *J. Chem. Eng. Data 13*, 179.

O'Donnell, M. E., & Williams, C. H., Jr. (1985) *Biochemistry 24*, 7617–7621.

Riddles, P. W., Blakeley, R. L., & Zerner, B. (1979) *Anal. Biochem. 94*, 75–81.

Swank, R. T., & Munkres, K. D. (1971) *Anal. Biochem. 39*, 462–477.

Szajewski, R. P., & Whitesides, G. M. (1980) *J. Am. Chem. Soc. 102*, 2011–2026.

Toniolo, C., Bonora, G. M., Vita, C., & Fontana, A. (1978) *Biochim. Biophys. Acta 532*, 327–336.

Weber, U., & Hartter, P. (1974) *Hoppe-Seyler's Z. Physiol. Chem. 355*, 189–199.

Williams, D. E., & Reisfeld, R. A. (1965) *Ann. N.Y. Acad. Sci. 121*, 373–381.

Yamamoto, M., & Ikenaka, T. (1967) *J. Biochem. (Tokyo) 62*, 141–149.